LIBRA–A Light Ion Beam Fusion Reactor Conceptual Design

G.A. Moses, G.L. Kulcinski, D. Bruggink, R. Engelstad, E. Lovell, J. MacFarlane, Z. Musicki, R. Peterson, M. Sawan, I. Sviatoslavsky, L. Wittenberg, G. Kessler, U. von Möllendorff, E. Stein, I. Smith, P. Corcoran, H. Nishimoto, J. Fockler, D. Cook, R. Olson

July 1988

UWFDM-787

FUSION TECHNOLOGY INSTITUTE

UNIVERSITY OF WISCONSIN

MADISON WISCONSIN

LIBRA–A Light Ion Beam Fusion Reactor Conceptual Design

G.A. Moses, G.L. Kulcinski, D. Bruggink, R. Engelstad, E. Lovell, J. MacFarlane, Z. Musicki, R. Peterson, M. Sawan, I. Sviatoslavsky, L. Wittenberg, G. Kessler, U. von Möllendorff, E. Stein, I. Smith, P. Corcoran, H. Nishimoto, J. Fockler, D. Cook, R. Olson

Fusion Technology Institute
University of Wisconsin
1500 Engineering Drive
Madison, WI 53706

http://fti.neep.wisc.edu

July 1988

UWFDM-787

LIBRA-A LIGHT ION BEAM FUSION REACTOR CONCEPTUAL DESIGN

G.A. Moses, G.L. Kulcinski, D. Bruggink, R. Engelstad,
E. Lovell, J. MacFarlane, Z. Musicki, R. Peterson,
M. Sawan, I. Sviatoslavsky, L. Wittenberg
University of Wisconsin Fusion Technology Institute
and Fusion Power Associates

G. Kessler, U. von Möllendorff, E. Stein
Kernforschungszentrum Karlsruhe

I. Smith, P. Corcoran, H. Nishimoto, J. Fockler
Pulse Sciences, Inc.

D. Cook and R. Olson
Sandia National Laboratory

ABSTRACT

The LIBRA light ion beam fusion commercial reactor study is a self-consistent conceptual design of a 330 MWe power plant with an accompanying economic analysis. Fusion targets are imploded by 4 MJ shaped pulses of 30 MeV Li ions at a rate of 3 Hz. The target gain is 80, leading to a yield of 320 MJ. The high intensity part of the ion pulse is delivered by 16 diodes through 16 separate z-pinch plasma channels formed in 100 torr of helium with trace amounts of lithium. The blanket is an array of porous flexible silicon carbide tubes with $Li_{17}Pb_{83}$ flowing downward through them. These tubes (INPORT units) shield the target chamber wall from both neutron damage and the shock overpressure of the target explosion. The target chamber is a right circular cylinder, 8.7 meters in diameter. The target chamber is "self-pumped" by the target explosion generated overpressure into a surge tank partially filled with liquid that surrounds the target chamber. This scheme refreshes the chamber at the desired 3 Hz frequency without excessive pumping demands. The blanket multiplication is 1.2 and the tritium breeding ratio is 1.4. The direct capital cost of LIBRA is estimated to be $2200/kWe.

INTRODUCTION

The LIBRA study is a self-consistent conceptual design of a light ion driven commercial fusion power reactor. Past LIB reactor designs include UTLIF [1], ADLIB [2] and EAGLE [3]. A major goal of the LIBRA study is to understand the potential of light ion fusion as the basis for small yet economically attractive power reactors. This is done by completing a self-consistent point design, evaluating its cost, and cost scaling the design to different power levels. Specific design parameters for LIBRA are given in Table I. A schematic of the reactor chamber design is shown in Figure 1.

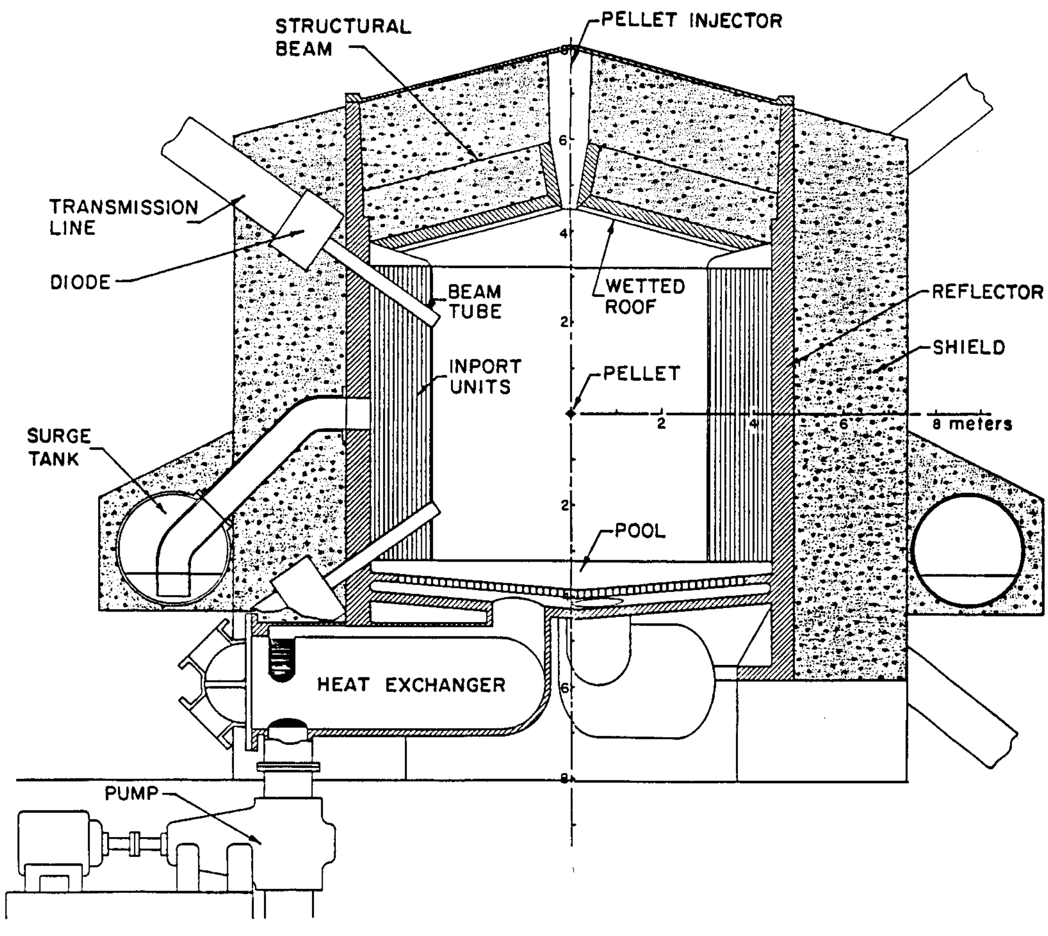

Figure 1. Cross section of LIBRA target chamber.

TARGET AND DRIVER PERFORMANCE

The target for LIBRA, depicted in Figure 2 in its ignition configuration, is a generic single shell design similar to that used in the HIBALL study [4]. The gain of 80 is consistent with recently published gain curves for heavy ion targets [5]. The LIBRA target is illuminated by two low power ion beams and 16 high power beams that combine on the target in a shaped pulse. The beams are

Table I. LIBRA Parameters

General		**Lithium Ion Beams**	
Net electric power	331 MW	Energy	25-35 MeV
Gross electric power	441 MW	Number high power	16
Thermal power	1160 MW	low power	2
Recirc. power fraction	0.25	Peak power on target	400 TW
Driver efficiency	0.23	Pulse compression ratio	5
Target gain	80	Pulse length on target	9 ns
Fusion gain	18.4	Current/channel	0.3 MA
Direct capital cost	$2200/kW	Entering on target	1.1 MA
Target Performance		Ion energy transport eff.	0.63
DT mass	3.2 mg	**Laser-Guided, Free Standing Channels**	
Input energy	4 MJ	Length	5.4 meters
Yield	320 MJ	Radius	0.5 cm
X-ray yield	67 MJ	Peak B-field	27 kG
Neutron yield	218 MJ	Peak current	100 kA
Endoergic loss	7 MJ	Rise time	1 μs
Neutron mult.	1.02	Voltage drop	1 MV
Applied-B Diode		**Cavity**	
Anode source	Liquid Li	Gas pressure	100 torr He
Anode current density	5 kA/cm^2	Radius to first surface	3 meters
Anode radius	8.4 cm	Pumping time	300 ms
Focal length	70 cm	Impulse on INPORTs	150 Pa-s
Microdivergence	5 mrad	Vaporized LiPb mass	9 kg
Macrodivergence	120 mrad	**INPORT Tube Blanket**	
Conversion efficiency	0.80	Tube material	SiC
Helia Pulsed Power		Packing fraction	0.33
Waterline energy	11.1 MJ	Coolant/breeder	$Li_{17}Pb_{83}$
No. of cells/module	26	Li-6 enrichment	90%
Voltage/cell	1.15 MV	Thickness	1.35 meters
Cell diameter	2.9 meters	Energy mult.	1.2
Module diameter	5.15 meters	Tritium breeding ratio	1.4
Module length	14.4 meters	**Tritium**	
PFL output voltage	1.15 MV	Inventory target prep.	696 g
Impedance	3 Ω	breeder	187 g
Dielectric	water	Effluent	10 Ci/day
Switch type	metglas saturable reactor		

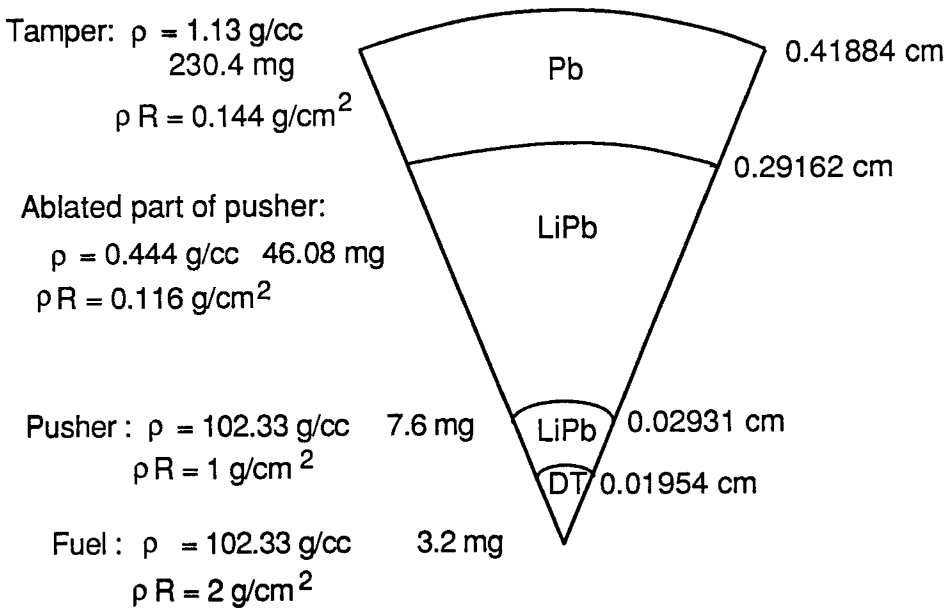

Figure 2. LIBRA target in ignition configuration.

positioned axisymmetrically at a half-angle of 35° according to the illumination prescription of Mark [6].

The target yield of 320 MJ and fractional burnup of 30% demand a burn time ρr of 3 g/cm^2. The fuel is compressed to 2 g/cm^2 while the surrounding low Z tamper provides the additional 1 g/cm^2. No detailed implosion calculations were done, but the energetics of the fuel payload mass and input energy and power are consistent with standard design criteria.

The design of the pulsed power driver [7], the repetitive diode [8], and the plasma channel transport [9] are described in companion papers in these proceedings. The overall efficiency of energy delivery to the target is 23%. This is shown in the power flow diagram in Figure 3. Combined with a target gain of 80, this gives a fusion gain (driver efficiency x target gain) of 18.4.

ION DIODE AND BEAM TRANSPORT

The pulsed power is converted into beams of ions that are transported to the target in free standing laser-guided discharge plasma channels. This feature has led us to diode and channel design concepts that call upon technologies that are still under development.

The ion diodes must be rep-rateable and with an extraction geometry. The LIBRA diode concept is an applied magnetic field extractor diode with an annular anode made of a porous material that is continuously wetted with liquid lithium. Recent experiments at Sandia National Laboratory show promise for this concept in barrel geometry single shot applied magnetic field diodes [10]. There is

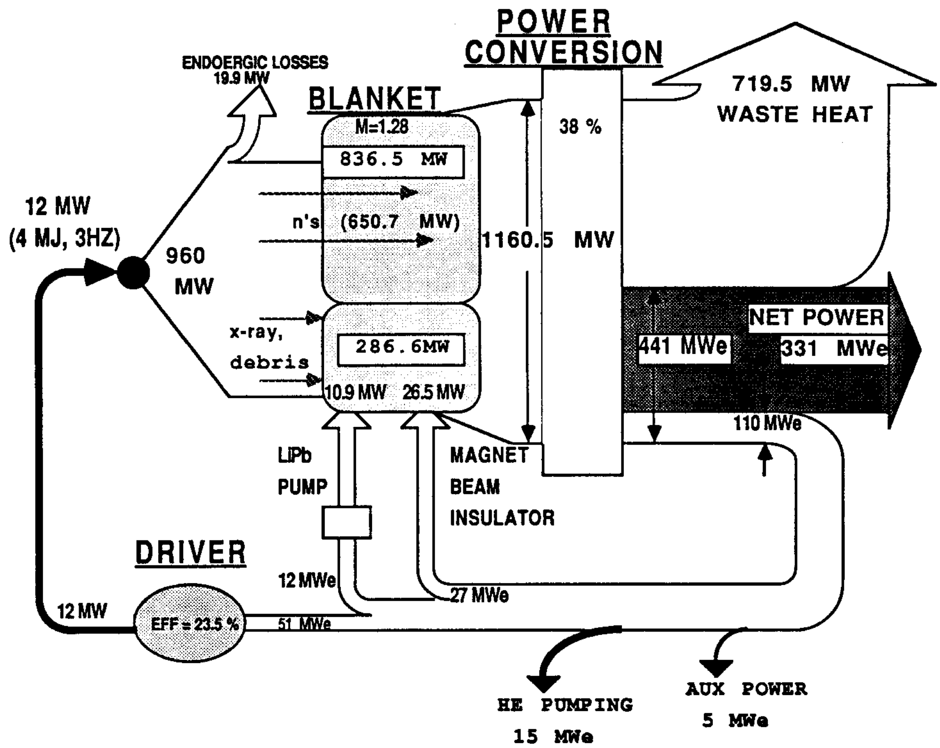

Figure 3. Power flow diagram.

currently work in progress on extractor and rep-rateable diodes (for example, the work at Cornell [8]). The lithium provides both a constantly replenished ion source and a means of carrying away the heat of diode electrons. The ion source density and microdivergence are extrapolations to what may be achieved in the future.

Plasma channels for transporting ions from the diodes to the target must also be created repetitively. This means that any structural parts of the channels, such as final focusing elements, that are near enough to the target explosion to be destroyed will have to be replaced before the next shot. We have approached this problem by proposing channels that are free-standing in a background gas and are created with laser-guided discharges, and therefore have no structures near the target. The channels would carry 63% of the ion beam energy to the target. Breakdown between the channels and INPORT tubes in the target chamber will be controlled with applied magnetic fields. We have analyzed the formation and performance of plasma channels [9] and believe that, even though work needs to continue in this area, there are no issues that would clearly exclude this beam transport concept.

CAVITY RESPONSE

Radiation-hydrodynamics calculations have been performed using the CONRAD computer code to study the conditions near the INPORT tubes after the target explosion. The primary concerns for the LIBRA design are: (1) the impulse given to the INPORT tubes due to the fireball-driven shock front and the recoil caused by vaporization of LiPb from the outer surface of the tubes; and (2) the LiPb condensation time, which must be shorter than the time between shots. Figure 4 shows the mass of LiPb in the vapor phase as a function of time after the target explosion. Approximately 80% of the target X-ray energy is deposited in the LiPb coating on the INPORT tubes, causing the immediate vaporization of roughly 7 kg. Between 10^{-7} and 10^{-5} seconds, additional vaporization occurs as radiation from the microfireball is deposited at the tubes. By 10 ms, the LiPb vapor mass drops from a peak of 9 kg down to 0.8 kg, which corresponds to a LiPb/He number ratio of 0.007. We therefore expect the repetition rate will not be constrained by the LiPb condensation time.

The impulse given to the INPORT tubes is approximately 150 Pa-s/shot. This is almost entirely due to the vaporization-induced recoil impulse. The shock ahead of the microfireball contributes little because it is overwhelmed by the

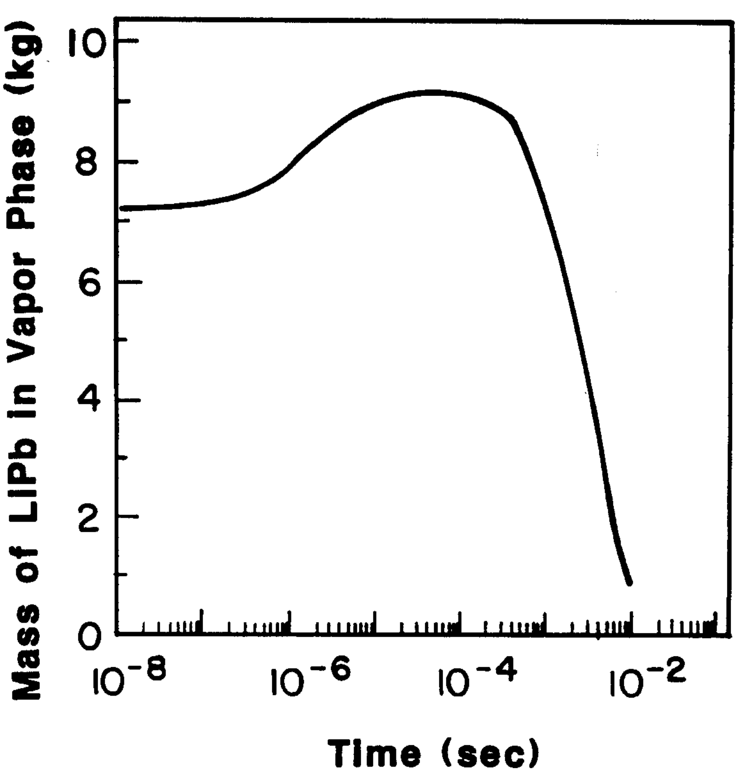

Figure 4. LiPb vapor mass vs. time.

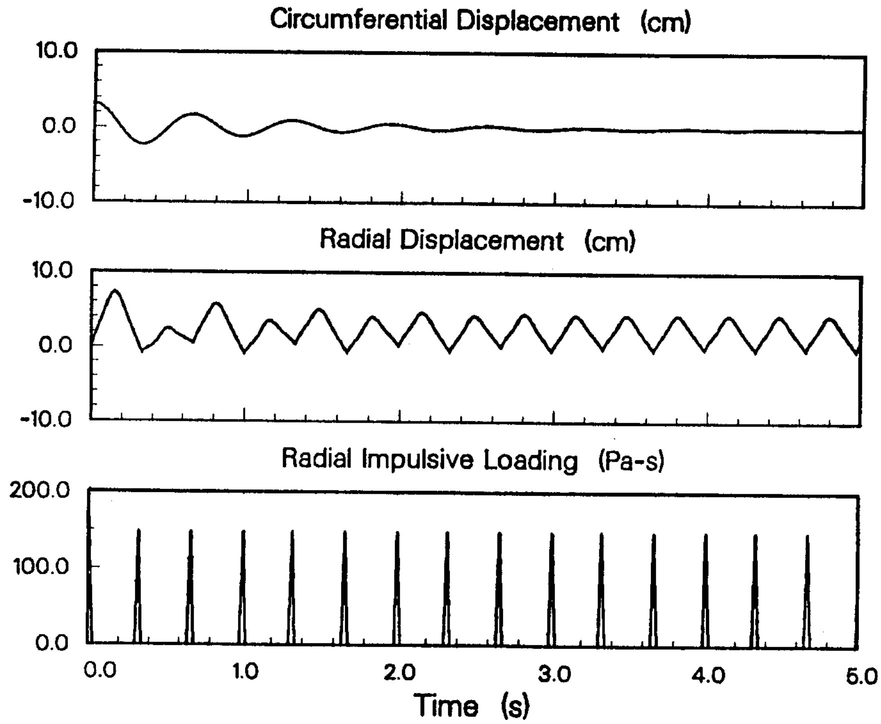

Figure 5. INPORT unit response.

vaporization front. The repetitive impulsive loading will produce dynamic motion of the first row of INPORTs. The determination of this mechanical response is necessary for radial placement of the tubes as well as identifying potential interference problems from circumferential movement. A comprehensive numerical simulation program has been developed which includes effects such as axial preload, tension gradient, flow velocity, length, diameter, dissipation, rep-rate and nonlinear displacement effects which are essential for modelling three dimensional motion. For all cases, the sequential impulses are applied radially, i.e., planar for each INPORT. It has been found that persistent radial and circumferential (orbital) motion is possible for some designs. However, for particular choices of physical parameters (e.g., flow velocity and pretension) the steady-state motion will be strictly planar, the preferred response. Figure 5 shows such results. The planar impulses of 150 Pa-s at 3 Hz produce radial displacements with a maximum startup value of 7 cm and a steady-state peak of 4 cm. The circumferential displacement has an initial perturbation which quickly dissipates. The INPORT length, diameter, and wall thickness are 6.4 m, 3 cm and 2 mm, respectively, and with a mean tension of 3000 N, the wall stresses are well below current strength levels of silicon carbide fiber.

TARGET CHAMBER DESIGN

The target chamber is a vertical cylinder with a slanting roof. The roof and sides of the chamber are covered with SiC fabric passages through which LiPb coolant/breeder flows collecting in a pool at the bottom of the chamber. Coolant seeping through the porous SiC fabric on the roof and the sides, and the bottom pool provide liquid protection against the surface heat emanating from the target. The deep penetrating neutrons deposit their energy within the bulk of the blanket and reflector components of the chamber.

Figure 1 is a cross section of the LIBRA chamber. The INPORT units are at a radius of 3 m from the target and occupy a zone up to a radius of 4.35 m at a 33% volumetric fraction. The front two rows are 3 cm and the remaining 9 rows are 10 cm in diameter respectively. They are followed by a 50 cm thick LiPb cooled steel reflector which is the primary structural component of the chamber. It is followed by a 2.5 m thick He gas cooled concrete shield.

There are nine equally spaced beam tubes on the top and an equal number on the bottom penetrating between the INPORT units at a 35° angle to the horizontal. The beam tubes are made of TZM coils which provide magnetic insulation for the plasma channels by generating a 3.2 T field within the tubes. At the reflector midplane, there are nine equally spaced 0.75 m diameter exhaust ducts leading to a toroidal suppression tank attached to the outer perimeter of the chamber. The post shot plasma in the chamber expands into the suppression tank where vacuum pumps evacuate it to maintain the needed operating conditions.

The bottom pool drains through a perforated plate which also acts as a shock absorber. The LiPb then goes to three heat exchangers built into the base of the chamber and then exits to be recycled through again. Helium gas circulating through the tubes of the heat exchanger then carries the energy to a conventional steam power cycle.

The chamber roof is at 7.7 m at its highest point above the pool and slants at 15°. It is designed to be taken apart for providing access to the inside of the chamber for maintenance purposes. The SiC fabric passages are attached to a 0.25 m thick LiPb cooled steel conical reflector which is welded to six equally spaced structural beams. This structure provides the support for the roof shield segments. At its center is a hub which holds the pellet injector. The last element in the roof is a flange which is the vacuum boundary for the chamber. When this flange is removed, the roof can be dismantled by removing the shield in six separate segments, then the reflector as a single unit, as shown in Figure 6. A 100 tonne crane is needed to accomplish this task.

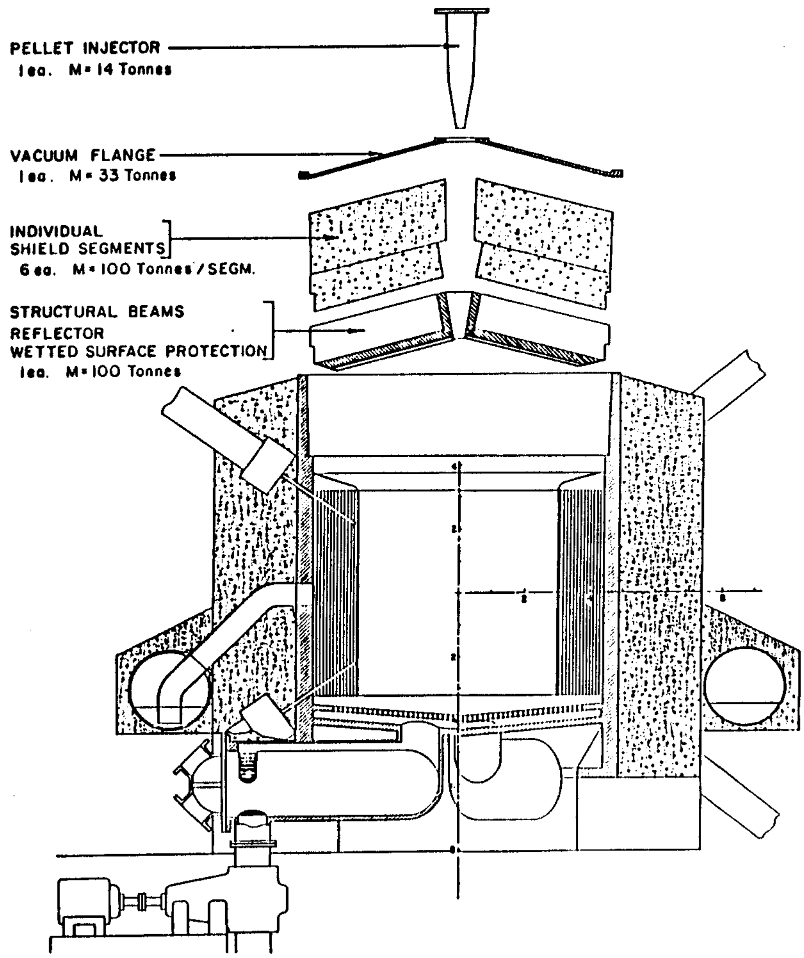

Figure 6. Disassembly of target chamber.

BLANKET RESPONSE

A one-dimensional (1-D) scoping analysis was performed to determine the blanket design options that satisfy the tritium breeding and wall protection requirements. A point source emitting neutrons and gamma photons with the spectra calculated for the LIBRA target was used at the center of the 3 m radius cavity. A minimum tritium breeding ratio (TBR) of 1.1 is required to achieve tritium self-sufficiency. The peak end-of-life atomic displacements (dpa) in HT-9 is required to not exceed 200 dpa implying that for 30 full power year (FPY) reactor life the peak dpa rate should not exceed 6.6 dpa/FPY. In addition, the blanket thickness needs to be minimized to minimize the length of the channels used for beam propagation.

Calculations were performed for different blanket thicknesses and ^{6}Li enrichments. The TBR and dpa rate values are mapped in Figure 7. The design point should be in the box indicated in the upper left corner. In order to

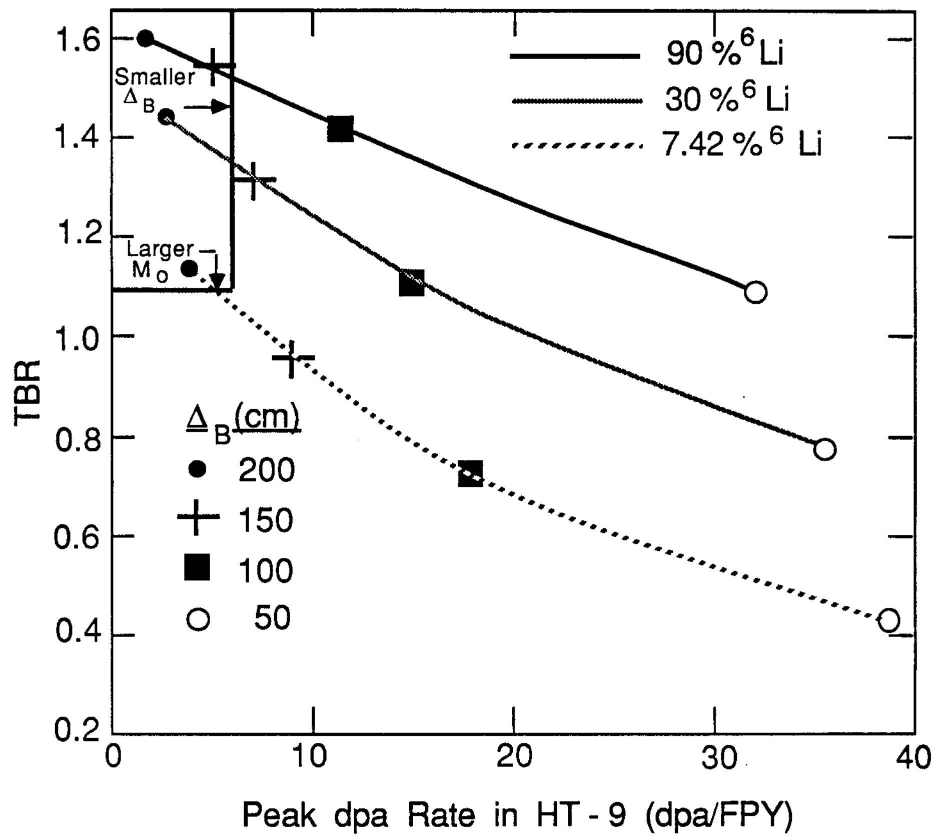

Figure 7. Tritium breeding ratio and damage rate.

satisfy the other design goals of minimizing the blanket thickness and maximizing M, it is clear that the design point should be at the right or lower boundaries of the box. The intersection of the boundaries of the box with the curves that correspond to different enrichments give the options that satisfy the design requirements. To minimize the length of the beam propagation channel, a 1.35 m thick blanket with 90% ^{6}Li enrichment is used in LIBRA, leading to local (1-D) TBR and M of 1.5 and 1.18, respectively. Since this results in a relatively large TBR in the chamber sides, a smaller local TBR is allowed in the reactor roof. A scoping analysis for the roof leads to a 10 cm thick $Li_{17}Pb_{83}$ protective layer followed by a 25 cm thick $Li_{17}Pb_{83}$ cooled HT-9 reflector. The local TBR in this zone is 0.8 and the peak dpa rate in HT-9 is 50 dpa/FPY implying that the roof structure needs to be replaced every 4 FPY. Since only ~ 14% of the source neutrons go to the roof, this design will yield an overall TBR that exceeds the minimum requirement by an adequate margin. Detailed three-dimensional neutronics calculations are underway to determine the overall nuclear parameters for the reactor.

TRITIUM FUELING, BREEDING AND INVENTORY

Hollow organic polymer shells are filled remotely in a pressure chamber with molecular DT and are subsequently overcoated mechanically with Pb foil. Batches of targets are stored at 19.8 K for 2 hours while a uniform thickness of solid DT forms on the interior surface of the polymer shell [11]. The uniformity of the fuel coating is caused by the radioactive induced sublimation of the DT [11]. A one-day's supply of fuel targets is maintained.

In order to limit the loss of tritium to < 10 Ci/d at the steam generator, tritium removal is accomplished from both the liquid metal and the helium circuits. Tritium in the helium circuit is converted to the oxide and is adsorbed on a desiccant.

The liquid breeder alloy within the reactor cavity contains the tritium formed during breeding plus the unburned DT from each target explosion. The tritium concentration in this liquid alloy is controlled by the diversion of 6.3 m^3/s of the alloy to a Tritium Removal System (TRS) [12]. By this technique the average tritium partial pressure in the alloy is maintained at 1.3×10^{-2} Pa and a concentration of 1.4×10^{-4} wt.ppm.

Tritium solubility in the SiC fibers of the INPORT tubes is estimated to yield an inventory of 150 g of tritium.

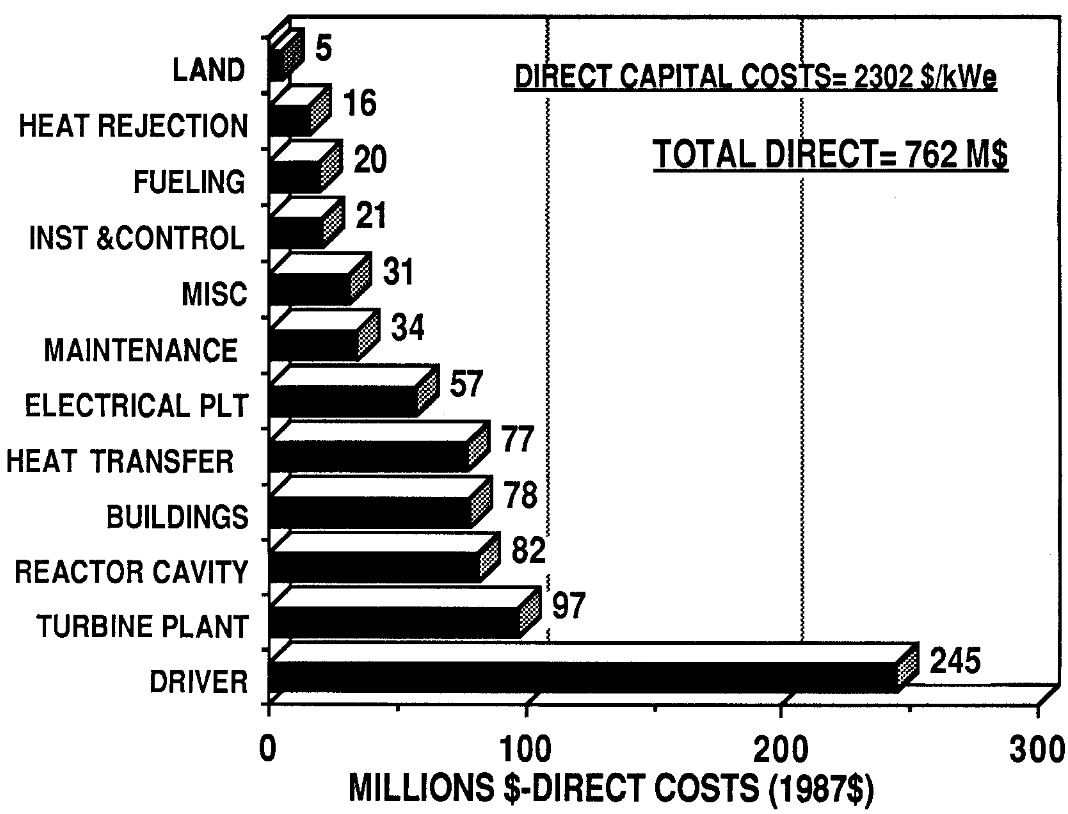

Figure 8. Direct capital costs of LIBRA.

LIBRA ECONOMICS

An important measure of the flexibility in the light ion beam fusion concept is the cost of electricity from such a power plant even at the relatively low power level chosen for this study (330 MWe). The details of the costing analysis will be given in the final report and Figure 8 summarizes the direct costs for the major components of LIBRA. The first obvious point is that the capital costs are dominated by the driver (32%) and 4 of the next 5 cost items (the turbine plant, buildings, heat transfer legs, and electrical plant) which depend more on the "conventional" power level, constitute another 41%. The reactor cavity only accounts for 11% of the total capital costs.

It is interesting to compare the LIBRA direct capital costs to those calculated for other fusion reactor designs published over the past 15 years (all normalized to 1987$). Figure 9 shows this comparison of LIBRA versus heavy ion beam reactors (HIBALL I and II) as well as for 8 other magnetic fusion devices. In general, all the other reactors are in the 1000 MWe level except for the HIBALL series which is in the 4000 MWe range. The main point from Figure 9 is that light ion beam fusion compares favorably to previous magnetic and heavy ion beam designs and that if the economy of scale can be applied to large LIB systems, the total direct cost may be even be less.

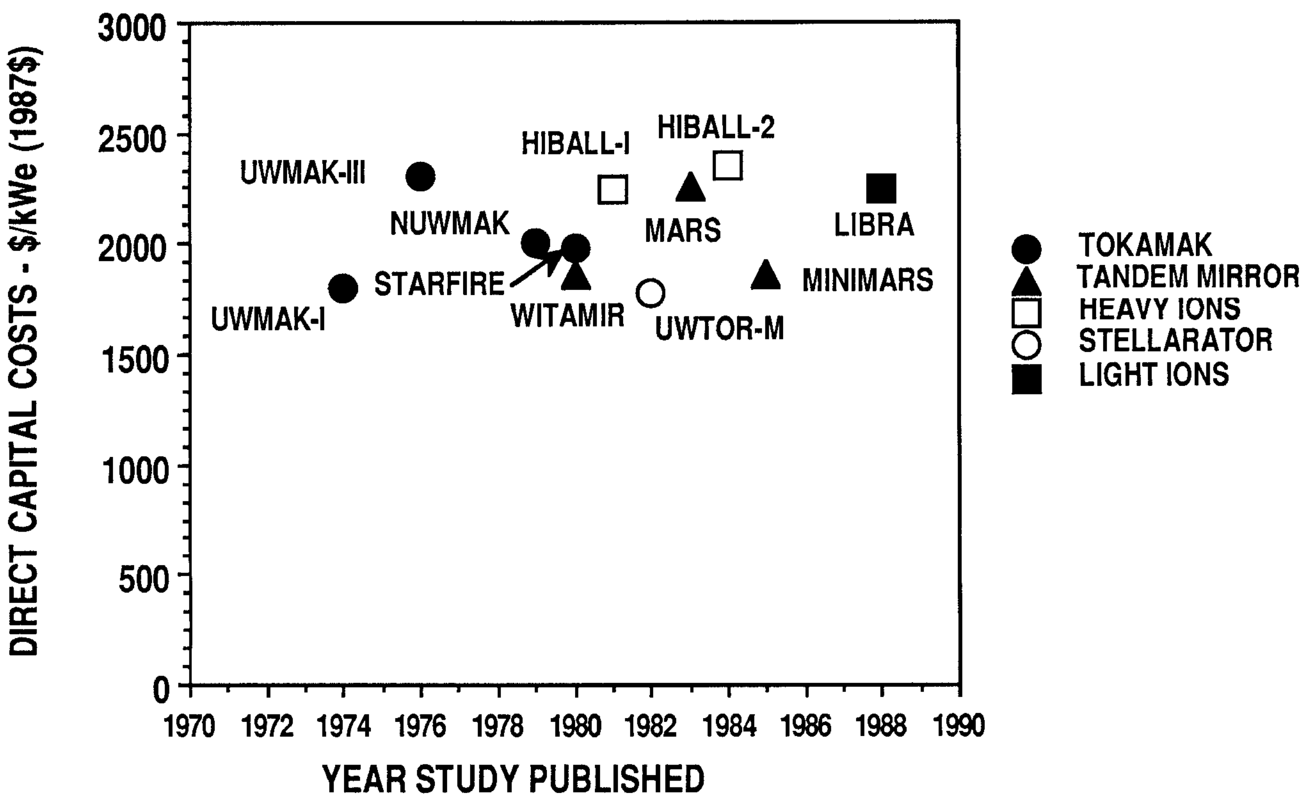

Figure 9. Comparison of LIBRA and other fusion designs.

ACKNOWLEDGEMENT

This work was supported by Kernforschungszentrum Karlsruhe and Sandia National Laboratory Albuquerque. Computer calculations were supported by the National Science Foundation at the San Diego Supercomputer Center.

REFERENCES

1. "Preliminary Design of Light Ion Beam Fusion Reactors, UTLIF (1) & ADLIB-1," University of Tokyo Nuclear Engineering Research Laboratory UTNL-R-0135 (1982).

2. K. Niu and S. Kawata, "Proposal of Power Plant by Light Ion Beam Fusion," Fusion Technology 11, 365 (1987).

3. "Light Ion System Analysis and Design-Phase I: Engineering Test Reactor Goal Specification," Research Project 1527, Electric Power Research Institute, April 1982 (no author).

4. D. Bohne, et al., "HIBALL-A Conceptual Design Study of a Heavy-Ion Driven Inertial Confinement Fusion Power Plant," Nucl. Engr. and Design 73, 195 (1982).

5. R.O. Bangerter, "Targets for Heavy Ion Fusion," Fusion Tech. 13, 348 (1988).

6. James W.-K. Mark, "Near Spherical Illumination of Ion-Beam and Laser Targets," Physics Letters 114A, 458 (1986).

7. I. Smith, "Conceptual Design of a Driver for LIBRA," to appear in these proceedings.

8. J. Greenley, "Concepts for Repetitive Ion Diodes", to appear in these proceedings.

9. R.R. Peterson and G.A. Moses, "Plasma Channels for the Propagation of Ion Beams in LIBRA," to appear in these proceedings.

10. K.W. Beig, et al., "Lithium Ion Source Experiments on PBFA II," 1988 IEEE Conference on Plasma Science (June 1988, Seattle, Washington) paper 1D7.

11. J.K. Hoffer and L.R. Foreman, "Radioactively Induced Sublimation in Solid Tritium," Phys. Rev. Letters, 60, 1310 (1988).

12. K.E. Plute, E.M. Larsen and L.J. Wittenberg, "Tritium Recovery from Liquid Lithium-Lead by Vacuum Degassing," Nuclear Tech./Fusion 4, 407 (1983).